Journal of Molecular Catalysis A: Chemical 317 (2010) 19–26

Contents lists available at ScienceDirect

Journal of Molecular Catalysis A: Chemical

journal homepage: www.elsevier.com/locate/molcata

Coordination chemistry studies and peroxidase activity of a new artificial metalloenzyme built by the "Trojan horse" strategy

Quentin Raffy, Rémy Ricoux, Elodie Sansiaume, Stéphanie Pethe, Jean-Pierre Mahy*

Equipe de Chimie Bioorganique et Bioinorganique, Institut de Chimie Moléculaire et des Matériaux d'Orsay, UMR CNRS 8182, Université Paris XI, 91405 Orsay Cedex, France

ARTICLE INFO

Article history:
Received 31 August 2009
Accepted 9 October 2009
Available online 20 October 2009

Keywords:
Artificial metalloenzymes
Metalloporphyrins
Catalysis
Peroxidase activity
Hybrid biocatalysts

ABSTRACT

In the general context of green chemistry, a considerable research effort is devoted to the elaboration of new artificial metalloproteins that catalyze, under mild conditions, the oxidation of a wide range of organic compounds, using cheap and environmentally friendly oxidants. A new artificial hemoprotein was obtained by the so-called "Trojan horse" strategy involving the non-covalent insertion of a cationic iron–porphyrin–estradiol cofactor into an anti-estradiol antibody. UV–vis titrations showed the formation of a 1/2 antibody/cofactor complex with a dissociation constant $K_D = 4.10^{-7}$ M. UV–vis determination of the Fe-imidazole binding constants showed that the protein provided a weak steric hindrance around the iron–porphyrin cofactor. The antibody–estradiol–iron–porphyrin complex displayed a peroxidase activity and catalyzed the oxidation of ABTS by H_2O_2 with about double the efficiency of the iron–porphyrin–estradiol alone. Kinetic studies revealed that this was due to a faster formation of the intermediate high valent iron–oxo species in the presence of the antibody protein. Consequently, the association of an anti-estradiol antibody with an iron–porphyrin–estradiol cofactor leads to a new artificial hemoprotein with an interesting peroxidase activity and the "Trojan horse" strategy appears as a valuable method to generate artificial metalloenzymes that could act as biocatalysts for selective oxidations.

1. Introduction

The development of ecologically friendly processes following the 12 principles of "green chemistry" defined by Anastas and Kirchhoff [1] has been a growing field in the chemical industry during the past years. One of these principles is the use of selectively catalyzed processes instead of stoichiometric ones, to minimize waste formation. The two main methods used industrially are biocatalysis and homogeneous catalysis, which are in many aspects complementary; while the enzymes work under mild conditions with high regioselectivity, synthetic catalysts are more widely applicable and accept a wider range of substrates. The construction of hybrid biocatalysts combining the best aspects of both the above-mentioned types of catalysts is a growing field, within which artificial metalloenzymes are especially developed. In particular, a huge interest has been devoted to the elaboration of artificial metalloenzymes that display a peroxidase activity, since such biocatalysts are able to perform the oxidation of a wide range of organic compounds of major interest in industrial fields such as food processing, bioremediation, etc using H_2O_2, which is a cheap and environmentally friendly oxidant [2].

Artificial metalloenzymes can be built by anchoring a metallic cofactor (responsible for the catalytic activity) in the cleft of a protein, either covalently or non-covalently. Among the non-covalent strategies, two major ones have been developed to obtain artificial metalloenzymes: the so-called "Host-guest" and "Trojan horse" strategies.

For the non-covalent anchoring of a cofactor into the cavity of a protein to lead to an artificial metalloenzyme able to induce reproducible enantioselectivity to the catalyzed reaction, the key feature is that the affinity of the protein for the cofactor be as high as possible. Artificial metalloenzymes have been obtained by this strategy with antibodies generated against metalloporphyrins, using their antigens as cofactors. Some have presented interesting peroxidase activities [3,4], and the association of an anti-microperoxidase 8 (MP8) antibody with its antigen was found able to catalyze the sulfoxidation of thioanisole by hydrogen peroxide with a good enantiomeric excess of 45% [5]. Recently, new artificial peroxidases have been built by association of xylanase A, from *Streptomyces lividans* with Fe(T*p*CPP). The studies performed have shown that the porphyrin was deeply inserted in the cleft of the protein, which brought steric hindrance around one of its faces [6]. The steric hindrance generated by the protein is an essential factor for inducing selectivity into the reaction catalyzed by the porphyrin. The artificial metalloprotein possessed a peroxidase activity and was able to catalyze enantioselectively the oxidation of sulfides into sulfoxides [7].

* Corresponding author. Tel.: +33 169 157 421; fax: +33 169 157 281.
E-mail address: jpmahy@icmo.u-psud.fr (J.-P. Mahy).

1381-1169/$ – see front matter © 2009 Elsevier B.V. All rights reserved.
doi:10.1016/j.molcata.2009.10.016

In the Trojan horse strategy, the cofactor is made of a metal complex, responsible for the catalytic activity, linked to a molecule presenting a high affinity for the host protein, in order to non-covalently anchor it into the protein. Wilson and Whitesides [8], and more recently Ward [9,10] have used this strategy with avidin or streptavidine as host proteins, and biotin metallo-conjugates as cofactors. This has led to artificial metalloenzymes capable of inducing excellent enantioselectivities into the catalyzed reaction.

Combining the use of antibodies as host proteins with the "Trojan horse" strategy, we built a new artificial metalloenzyme by association of the iron–porphyrin–estradiol conjugate **1** (Fig. 1) with the anti-estradiol antibody **7A3**, whose high affinity for its antigen ($K_D = 9.5 \times 10^{-10}$ M) [11] made it an excellent candidate for the elaboration of a new artificial metalloenzyme. The new metalloenzyme was found to catalyze the sulfoxidation of thioanisole by H_2O_2 with a moderate enantiomeric excess [12].

In order to validate the concept of constructing artificial metalloenzymes by association of an antibody with an antigen-linked metal complex, we wanted to better characterize our system. Here we present a study on the structure and peroxidase activity of such a system, the results of which will be very helpful to design new artificial metalloenzymes with better activities and selectivities. UV–vis spectroscopy experiments were performed to evaluate the effect of the antibody on the artificial metalloenzymes, to determine the stoichiometry of the antibody–cofactor complex and its dissociation constant. Coordination studies with imidazole allowed us to measure the steric hindrance introduced by the protein around the iron–porphyrin cofactor. Finally, the peroxidase activity of the hemozyme was assessed, with ABTS as co-substrate, and compared to that of the cofactor alone by means of kinetic studies. Our results showed that the artificial metalloenzyme displayed a two-fold increase in peroxidase activity compared to the iron–porphyrin–estradiol alone. Kinetic studies showed a similar increase in the rate constant for the formation of the high valent iron–oxo species in the presence of the antibody compared to the iron–porphyrin–estradiol alone.

2. Material and methods

2.1. Physical measurements

UV–vis spectroscopy studies were performed on double beam UVIKON 860 XL and CARY 300 BIO VARIAN spectrophotometers.

^{1}H NMR spectrum were recorded in D_2O on a Bruker AM360 spectrometer.

2.2. Buffers

All buffers were prepared with bi-distilled water.

Buffer **A**: phosphate–citrate buffer pH 3 was prepared by mixing 79.5 mL of 0.1 M citric acid and 20.6 mL of a 0.2 M solution of Na_2HPO_4.

Buffer **B**: 50 mM phosphate buffer pH 7 was prepared by mixing 30.5 mL of a 0.05 M solution of Na_2HPO_4 and 19.5 mL of a 0.05 M solution of NaH_2PO_4.

Buffer **C**: 50 mM phosphate buffer pH 7.4 was prepared by mixing 40.5 mL of a 0.05 M solution of Na_2HPO_4 and 9.5 mL of a 0.05 M solution of NaH_2PO_4.

2.3. Synthesis of the estradiol–iron(III)metalloporphyrin cofactor 1

The iron(III) 5,10,15-tris(4-N-methylpyridiniumyl)-20-(4-phenyl(3-O-amidoxymethylestradiol)) porphyrin **1** (Fig. 1) was prepared as described previously [12] in two steps: coupling of 5,10,15-tris(4-pyridyl)-20-(4-aminophenyl) porphyrin with 3-O-carboxymethylestradiol followed by the insertion of the iron atom by reaction with $FeCl_2 \cdot 4H_2O$.

2.4. Preparation of the anti-estradiol antibody *7A3*

The antibody that was used as apoprotein was a monoclonal IgG, **7A3**, that was generated by immunization of mice with an antigen obtained by covalent linkage of estradiol in 3-position to BSA [11].

2.5. Characterization of the *1*–*7A3* complex

2.5.1. Comparison of the UV–vis spectrum of cofactor *1* with that of the *1*–*7A3* complex

A 5 μM solution of **1** in phosphate–citrate buffer pH 4.4 was prepared by mixing 12.5 μL of a 200 μM solution of **1** in buffer **A**, 250 μL of buffer **C**, 187.5 μL of buffer **A** and 50 μL of water. The 5 μM solution of **1**–**7A3** in phosphate–citrate buffer pH 4.4 was obtained in a similar way by replacing 250 μL of buffer **C** by 250 μL of a 25 μM solution of antibody **7A3** in buffer **C**.

The UV–vis spectra of both solutions were then recorded between 350 and 700 nm.

2.5.2. Titration of antibody *7A3* by a solution of cofactor *1*

Increasing amounts (from 0 to 3.5 molar equivalents) of a 200 μM solution of cofactor **1** in buffer **A** were added to a sample cuvette that contained a mixture of 260 μL of a 25 μM solution of antibody **7A3** in buffer **C** and 200 μL of buffer **A**. The absorbance $A_{\mathbf{1}\text{–}\mathbf{7A3}}$ was recorded between 250 and 700 nm, five minutes after each addition. The same experiment was performed with 260 μL of buffer **C** instead of the **7A3** solution, to measure the absorbance of the cofactor alone, $A_{\mathbf{1}}$. After correction of the dilution induced by the volume of cofactor added, the difference $\Delta A = A_{\mathbf{1}\text{–}\mathbf{7A3}} - A_{\mathbf{1}}$ at 394 nm was plotted as a function of the number of equivalents of **1** added. This allowed to determine the stoichiometry of the complex formed by **1** with the antibody **7A3**.

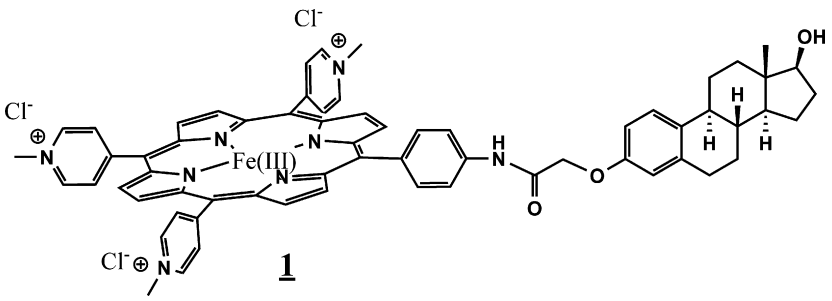

Fig. 1. Structure of the iron–porphyrin–estradiol conjugate 1 [12].

*2.5.3. Determination of the dissociation constant of the **1**–**7A3** complex*

To calculate the dissociation constant K_D of the cofactor **1**–**7A3** complex, the two estradiol-binding sites (S) of the antibody were considered as being independent from each other.

The dissociation constant K_D can then be written as follows:

$$K_D = \frac{[\underline{\mathbf{1}}] \cdot [S]}{[\underline{\mathbf{1}} - S]} \quad (1)$$

where $[S]$ stands for the concentration of the free recognition sites of the antibody, and $[\underline{\mathbf{1}} - S]$ for the concentration of recognition sites engaged in a complex with the cofactor **1**.

For each concentration of cofactor added to the antibody, the following two equations can be written:

$$[\underline{\mathbf{1}}]_0 = [\underline{\mathbf{1}}] + [\underline{\mathbf{1}} - S] \quad (2)$$

$$[S]_0 = 2 \cdot [\mathbf{7A3}] = [S] + [\underline{\mathbf{1}} - S] \quad (3)$$

where $[\underline{\mathbf{1}}]_0$ and $[S]_0$ stand for the initial cofactor and recognition site concentrations, respectively.

The dissociation constant K_D can then be written as a function of $[\underline{\mathbf{1}} - S]$:

$$K_D = \frac{([\underline{\mathbf{1}}]_0 - [\underline{\mathbf{1}} - S]) \cdot ([S]_0 - [\underline{\mathbf{1}} - S])}{[\underline{\mathbf{1}} - S]} \quad (4)$$

which gives:

$$[\underline{\mathbf{1}}]_0 = \frac{[\underline{\mathbf{1}} - S] \cdot K_D}{[S]_0 - [\underline{\mathbf{1}} - S]} + [\underline{\mathbf{1}} - S] \quad (5)$$

On the other hand, the absorbances $A_{\underline{\mathbf{1}}-\mathbf{7A3}}$ and $A_{\underline{\mathbf{1}}}$ measured for each of the two solutions follow the Beer–Lambert's law:

$$A_{\underline{\mathbf{1}}-\mathbf{7A3}} = \varepsilon_{\underline{\mathbf{1}}-S}[\underline{\mathbf{1}} - S] \cdot l + \varepsilon_{\underline{\mathbf{1}}}[\underline{\mathbf{1}}] \cdot l$$

$$A_{\underline{\mathbf{1}}} = \varepsilon_{\underline{\mathbf{1}}}[\underline{\mathbf{1}}]_0 \cdot l$$

As a result, ΔA can be linked to $[\underline{\mathbf{1}} - S]$ by the following equation:

$$\Delta A = A_{\underline{\mathbf{1}}-\mathbf{7A3}} - A_{\underline{\mathbf{1}}} = (\varepsilon_{\underline{\mathbf{1}}-S} - \varepsilon_{\underline{\mathbf{1}}}) \cdot [\underline{\mathbf{1}} - S] \cdot l$$

which gives:

$$[\underline{\mathbf{1}} - S] = \frac{\Delta A}{\varepsilon_{\underline{\mathbf{1}}-S} - \varepsilon_{\underline{\mathbf{1}}}} \quad (6)$$

The relation (5) then becomes:

$$[\underline{\mathbf{1}}]_0 = \frac{(\Delta A/\varepsilon_{\underline{\mathbf{1}}-S} - \varepsilon_{\underline{\mathbf{1}}})K_D}{[S]_0 - \Delta A/(\varepsilon_{\underline{\mathbf{1}}-S} - \varepsilon_{\underline{\mathbf{1}}})} + \frac{\Delta A}{\varepsilon_{\underline{\mathbf{1}}-S} - \varepsilon_{\underline{\mathbf{1}}}} = g\left(\frac{\Delta A}{\varepsilon_{\underline{\mathbf{1}}-S} - \varepsilon_{\underline{\mathbf{1}}}}\right) \quad (7)$$

$\varepsilon_{\underline{\mathbf{1}}-S}$ and $\varepsilon_{\underline{\mathbf{1}}}$ have been calculated with $A_{\underline{\mathbf{1}}-\mathbf{7A3}}$ and $A_{\underline{\mathbf{1}}}$, considering that for the first additions of cofactor, the absorption of the antibody–cofactor solution measured is that of the complex.

As a result, K_D can be estimated with a non-linear regression of $[\underline{\mathbf{1}}]_0$ with the function $g(\Delta A/(\varepsilon_{\underline{\mathbf{1}}-S} - \varepsilon_{\underline{\mathbf{1}}}))$.

*2.5.4. Coordination of imidazole on the iron atom of the cofactor **1**–antibody complex*

12.5 μL of a 200 μM solution of cofactor **1** in buffer **A** were added to a mixture of 250 μL of a 25 μM solution of antibody **7A3** in buffer **C**, 188.5 μL of buffer **A** and 50 μL of water, in a quartz sample cuvette. The final mixture was incubated at room temperature for 2 h. The reference cuvette contains 250 μL of buffer **C**, 200 μL of buffer **A** and 50 μL of water. Increasing amounts of a 1 M solution of imidazole in water were added to both cuvettes, so as to obtain final concentrations of imidazole between 0 and 91 mM. A difference UV–vis spectrum was recorded between 350 and 700 nm 3 min after each addition of imidazole, no further evolution of the spectrum being observed after that time.

*2.5.5. Effect of sodium hydroxide on cofactor **1** and on its complex with antibody **7A3***

12.5 μL of a 200 μM solution of cofactor **1** in buffer **A** were added to a mixture of 188.5 μL of buffer **A**, 50 μL of water, and either 250 μL of buffer **C**, to yield a 5 μM solution of **1**, or 250 μL of a 25 μM solution of antibody **7A3** in buffer **C**, to yield a 5 μM solution of **1**–**7A3**. Increasing volumes of a 1 M aqueous solution of NaOH, from 0 to 135 μL were then added to both solutions and UV–vis spectra were recorded between 350 and 700 nm after each addition.

2.6. Peroxidase activity assay

All the experiments were realized in thermostated cuvettes at 22.5 °C. For each experiment, auto-zero was made immediately before addition of H_2O_2.

2.6.1. Effect of the hydrogen peroxide concentration on the initial rate of oxidation of 2,2′-azino-bis(3-ethylbenzothiazoline-6-sulfonate) (ABTS)

*2.6.1.1. Cofactor **1** alone.* A 5 μM solution of **1** was prepared in a 500 μL quartz cuvette, by mixing 250 μL of buffer **C**, 187.5 μL of buffer **A** and 12.5 μL of a 200 μM solution of cofactor in buffer **A**. 25 μL of a 10 mM solution of ABTS freshly prepared in water were then added. X μL of water and $(25 - X)$ μL of a 12.6 or 25.2 μM aqueous solution of H_2O_2 were then successively added so as to obtain a final volume of 500 μL and final H_2O_2 concentrations ranging between 84 and 1700 μM. The H_2O_2 concentrations of the added solutions were checked by UV–vis spectrometry using an $\varepsilon_{H_2O_2}$ (240 nm) = 39.4 M^{-1} cm^{-1} [13].

The peroxidase reaction was initiated by the addition of H_2O_2, and the absorbance at 414 nm corresponding to the $ABTS^{\bullet+}$ radical cation was monitored as a function of time. Initial rates were calculated from a linear regression of the most linear part of the curve representing the absorbance at 414 nm as a function of time.

Due to the short duration of the recordings (about 20 min) and the high concentrations of $ABTS^{\bullet+}$ formed, the influence on the signal of the eventual variations in the absorbance of the catalyst at 414 nm could be neglected.

*2.6.1.2. Cofactor **1** in the presence of antibody **7A3**.* A mixture of 1.25 mL of a 25 μM solution of antibody in buffer **C**, 938 μL of buffer **A** and 62.5 μL of a 200 μM solution of cofactor **1** in buffer **A** (final concentrations: 5 μM in cofactor and 12.5 μM in antibody) were incubated for 2 h at room temperature. 450 μL of this mixture was then poured in the quartz sample cuvette, and 25 μL of a freshly prepared 10 mM solution of ABTS in water was then added. Water and hydrogen peroxide were added as described above, and the absorbance at 414 nm was monitored as a function of time.

2.6.2. Effect of the catalyst concentration on the initial rate of oxidation of 2,2′-azino-bis(3-ethylbenzothiazoline-6-sulfonate) (ABTS)

*2.6.2.1. Cofactor **1** alone.* Each solution was prepared in a 500 μL quartz cuvette, by mixing 250 μL of buffer **C**, 200 − X μL of buffer **A** and X μL of a 200 μM solution of cofactor **1** in buffer **A**, so as to obtain a final volume of 450 μL and cofactor **1** concentrations ranging between 1 and 10 μM. 25 μL of a 10 mM solution of ABTS freshly prepared in water were then added, followed by 25 μL of a 24 mM aqueous solution of H_2O_2.

The peroxidase reaction was initiated by the addition of H_2O_2, and the absorbance at 414 nm corresponding to the $ABTS^{\bullet+}$ radical cation was monitored as a function of time.

Initial rates were calculated from a linear regression of the most linear part of the curve representing the absorbance at 414 nm as a function of time.

*2.6.2.2. Cofactor **1** in the presence of antibody **7A3**.* Three solutions were prepared, mixing respectively 150, 100, 50 μL of a 25 μM solution of antibody **7A3** in buffer **C** with 100, 150, and 200 μL of buffer **C**, 192.5, 195, and 197.5 μL of buffer **A** and 7.5, 5, and 2.5 μL of a 200 μM solution of cofactor **1** in buffer **A**, so as to obtain in each case a volume of 450 μL, with cofactor **1** concentrations of 1, 2 and 3 μM, the **7A3**/**1** ratio remaining equal to 2.5.

25 μL of a 10 mM solution of ABTS freshly prepared in water were then added, followed by 25 μL of a 24 mM aqueous solution of H_2O_2. The peroxidase reaction was initiated as described above with the cofactor alone, by the addition of H_2O_2, and the absorbance at 414 nm corresponding to the $ABTS^{\bullet+}$ radical cation was monitored as a function of time.

2.6.2.3. Non-linear regressions. All non-linear regression obtained from experimental data were calculated with the CurveExpert program, version 1.3.

3. Results and discussion

3.1. Insertion of the cofactor in the antibody

The UV–vis spectrum of cofactor **1** was recorded in 0.1 M phosphate–citrate buffer pH 4.4 alone and in the presence of an excess of antibody **7A3** (2.5 equivalents, i.e. 5 binding site eq.) in order to favor the binding of the estradiol moiety of **1** inside the binding site of the antibody **7A3** (Fig. 2).

When comparing the two spectra, it appears that in the presence of the antibody, only a slight shift of the Soret band (1 nm) can be observed, together with an increase in its intensity. This is in agreement with the insertion of the porphyrin in a hydrophobic environment, with no amino-acid side chain acting as a fifth axial ligand of the iron. Such a phenomenon had already been observed by Cochran and Schultz for the insertion of iron(III)–mesoporphyrin IX into the hydrophobic cavity of the corresponding anti-N-methyl-mesoporphyrin IX monoclonal antibody [14]. This is also in agreement with the anchoring of cofactor **1** thanks to the specific recognition of the estradiol anchor by the antibody **7A3**, the amino acids located close to the binding site of the antibody having mostly hydrophobic side chains (Fig. 3).

In order to check the stoichiometry of the **1**–**7A3** complex and to calculate its dissociation constant, increasing amounts of cofactor were added to a 14.5 μM solution of antibody **7A3** in a 6/4 (v/v) mixture of 0.1 M phosphate buffer of pH 7.4 and phosphate–citrate buffer of pH 3. The same experiment was performed without the antibody, to measure the absorbance of the cofactor alone. The titration was followed by UV–vis spectroscopy as described in the Section 2, and the difference between the absorbances at 394 nm of the solution of cofactor added to the antibody and the one of the cofactor alone, $\Delta A_{394\,nm}$, was plotted against the **1**/antibody ratio (Fig. 4(a)). $\Delta A_{394\,nm}$ clearly increases linearly with the **1**/**7A3** ratio until 2 equivalents of cofactor **1** have been added to the antibody, and then reaches a plateau. This indicates that two cofactors are bound per antibody, which is in agreement with the binding of **1** to the antibody thanks to the specific recognition of its estradiol anchor by the antibody binding site.

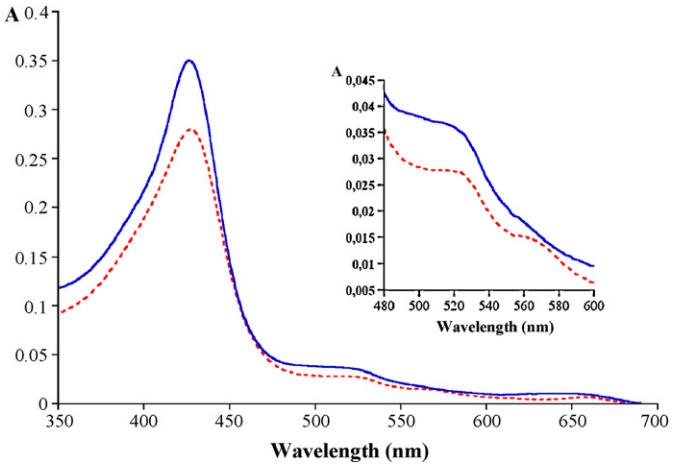

Fig. 2. Superimposition of the spectra of **1**, 5 μM in 0.1 M phosphate–citrate buffer, pH 4.4 alone (dashed line), and in the presence of 12.5 μM **7A3** (plain line).

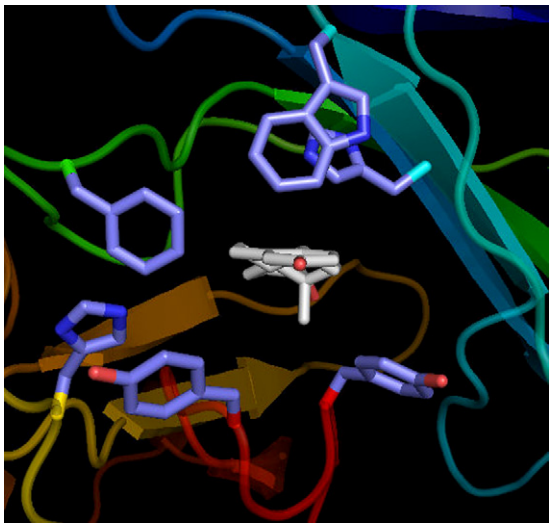

Fig. 3. Model structure of the estradiol-binding site of **7A3** Fab, with the antigen inside. Several hydrophobic residues can be seen at the entrance of the cavity. Side chains displayed (violet): Trp54, His52, Tyr101, Tyr98, His31 and Phe103. (For interpretation of the references to color in this figure legend, the reader is referred to the web version of the article.)

The function $g(\Delta A/(\varepsilon_{\mathbf{1}-S} - \varepsilon_{\mathbf{1}}))$, relating the concentration of cofactor **1** added with the absorbances measured (cf. Section 2), allows an estimation of K_D with a non-linear regression of the experimental data (see Section 2 and Fig. 4(b)). These last show a good fit to the function, and the dissociation constant is computed; $K_D = 4.0 \times 10^{-7}$ M. When compared to the dissociation constant of the antibody–antigen complex ($K_D = 9.5 \times 10^{-10}$ M), this value shows that the affinity of the antibody for the estradiol of the cofactor **1** has been lowered by only 2 orders of magnitude, despite the steric hindrance brought by the porphyrin. This confirms that in the presence of an excess of antibody, and for concentrations above micromolar, almost every molecule of cofactor **1** is accommodated in the antibody's pocket.

3.2. Active site topology

In order to examine the environment of the porphyrin macrocycle when **1** was bound to antibody **7A3**, and in particular the steric hindrance due to the amino-acid side chains, the binding of imidazole on the iron atom was studied at pH 4.4, both for **1** alone and for the **1**–**7A3** complex. To a solution of cofactor in the presence of an excess of antibody, increasing concentrations of imidazole were added, and UV–vis spectra of the resulting mixture were recorded (Fig. 5(a)).

As the cofactor is monomeric at pH 4.4, in the presence of the antibody, the equilibrium of the complexation can be written as in the following equation, with $n = 0$, 1 or 2.

$$\mathrm{PFe(III)} + n\,\mathrm{ImH} \rightleftharpoons \mathrm{PFe(III)(ImH)}_n$$

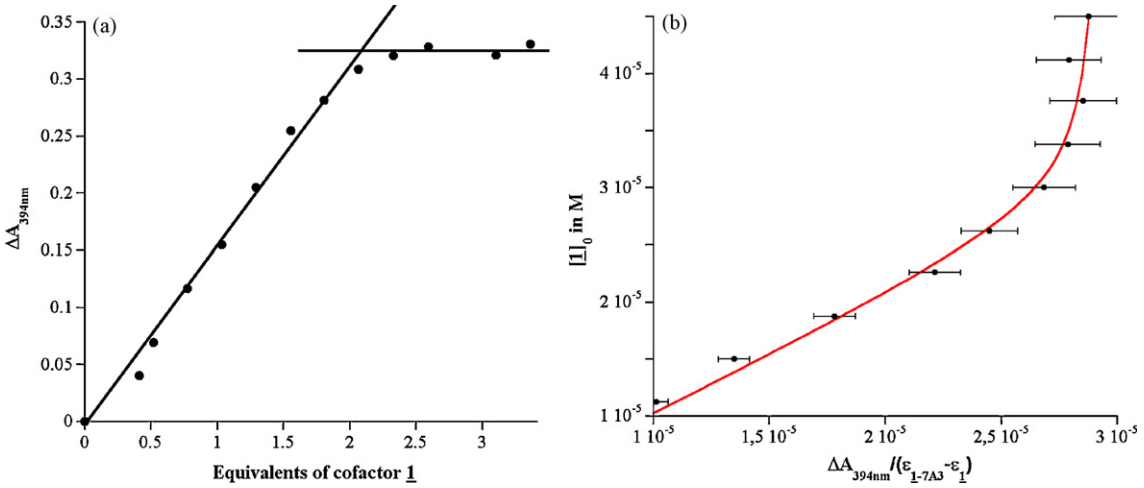

Fig. 4. (a) Variations of the differential absorbance at 394 nm as a function of the **1**/**7A3** ratio. [**7A3**] = 14.5 μM. (b) Concentration of cofactor added $[\underline{1}]_0$ as a function of $\Delta A/(\varepsilon_{\underline{1}\text{-}S} - \varepsilon_{\underline{1}})$. Dots: experimental data. Plain curve: non-linear regression with the function $g(\Delta A/(\varepsilon_{\underline{1}\text{-}S} - \varepsilon_{\underline{1}}))$.

The dissociation constant of the equilibrium can be written as:

$$K_D = \frac{[PFe(III)][ImH]^n}{[PFe(III)(ImH)_n]} \quad (8)$$

The spectral evolution observed involved the formation of well-defined isobestic points indicating the presence of two absorbing species. According to Brault and Rougee [15], it can then be analyzed by means of the standard equation:

$$\frac{1}{\Delta A} = \frac{1}{\Delta A_\infty} + \frac{K_D}{[ImH]^n} \cdot \frac{1}{\Delta A_\infty} \quad (9)$$

where $\Delta A = A - A_0$ and $\Delta A_\infty = A_\infty - A_0$ and A_0, A_∞, and A are the absorbances of the initial, final and mixed species respectively. As a result, the quantity of imidazole bound per molecule of cofactor n and the dissociation constant K_D can be estimated from a polynomial regression of $1/\Delta A$ as a function of 1/[ImH].

As clearly shown in the graph of Fig. 5(b), which is based on the measurement of the absorbance at 553 nm of the complex formed, $1/\Delta A$ is accurately fitted by a second order polynomial function of 1/[ImH], indicating that despite the presence of the antibody, the iron of the porphyrin of **1** can be complexed by two imidazole molecules. The dissociation constant of the complex formed was also calculated, $K_D = 5.5.10^{-4} \pm 0.5.10^{-4}$ M^2, which gives a C_{50} of 23 mM. The dimerization of the cofactor **1** caused by an excess of imidazole prevents direct comparison of this dissociation constant to that which would be obtained in the absence of the antibody. However, the C_{50} found can be compared to the one measured under similar conditions with the *tetra*-paracarboxyphenyl porphyrin, which is seven times lower, with a value of 3.4 mM [3]. This shows that, even though the steric hindrance brought by the antibody around the porphyrin of the cofactor does not prevent the complexation of the iron by two imidazole molecules, it strongly penalizes it.

The dimerization of non sterically hindered iron porphyrins in basic medium—via the formation of a μ-oxo bridge—is a well-known phenomenon [16–18]. Such dimerization occurred with cofactor **1** above pH 5, which was demonstrated by NMR and UV–vis spectrometry, the dimeric species being characterized by a maximum of absorption at 572 nm (Fig. 6). To further investigate the steric hindrance generated by the antibody around the metallo-porphyrinic ring of the cofactor, the possible dimerization of the cofactor in presence of the protein has been studied.

Since the formation of μ-oxo bridges occurs in basic solutions, increasing quantities of sodium hydroxide were added to solutions

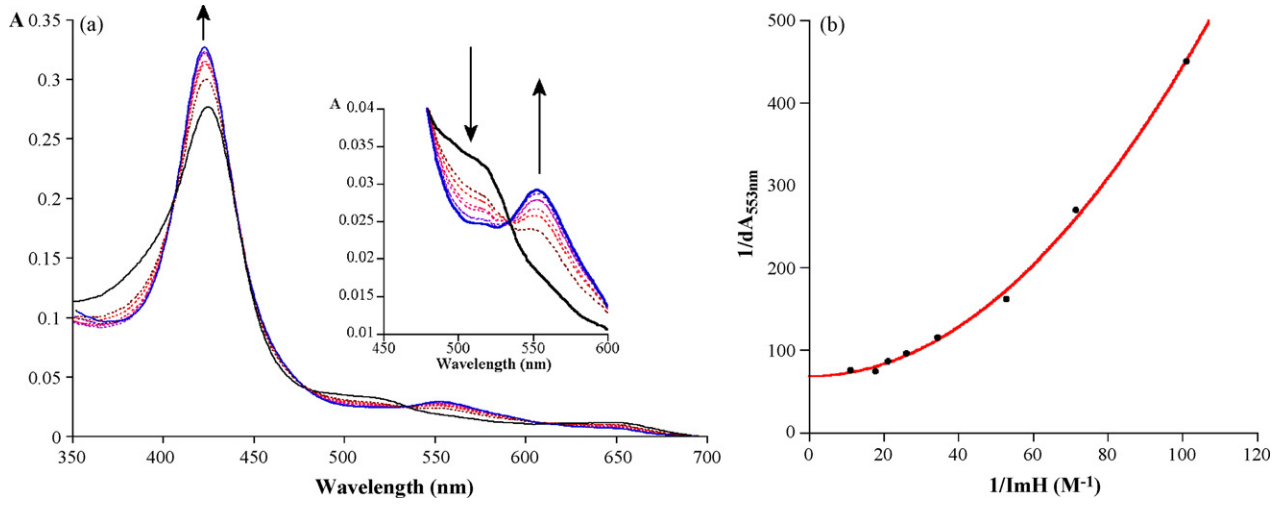

Fig. 5. (a) Superposed spectra obtained after the addition of increasing amounts of imidazole to a 500 μL solution of 5 μM **1** and 12.5 μM **7A3** in phosphate–citrate buffer, pH 4.4. Arrows indicate the direction of change of the various bands as a function of increasing imidazole concentration. (b) Graph representing $1/\Delta A$ at 553 nm as a function of 1/[ImH]. Plain line: second order polynomial fit.

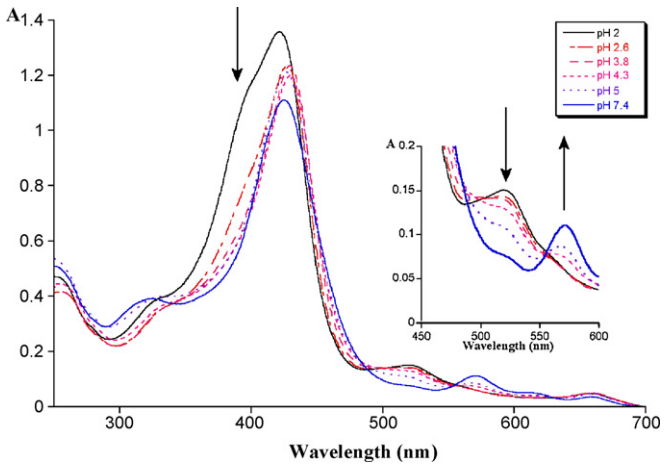

Fig. 6. Variations of the UV–vis spectrum of 20 μM iron(III)–porphyrin–estradiol conjugate **1** as a function of pH. The increase and decrease of the bands are indicated by arrows.

of cofactor in the presence of the antibody, and UV–vis spectra of the resulting solutions were recorded (Fig. 7(b)). The same experiment was also performed with the cofactor **1** alone (Fig. 7(a)).

The comparison of the two sets of spectra recorded (with and without the antibody) shows that the increase of pH has very different effects on the cofactor in the presence of the protein. Indeed, the spectrum of the cofactor alone shows a strong decrease of the absorbance with the increase of the pH, together with the disappearance of the maximum at 523 nm, and the increase of the peak at 572 nm. This can be explained by the combination of two effects: the precipitation of the cofactor, which causes the decrease of the signal intensity, together with the formation of the dimeric species, which presents a maximum at 572 nm. In the presence of the antibody, no maximum at 572 nm is observed, whatever the amount of sodium hydroxide added to the solution, and, instead of a diminution of the absorbance, we observe a refinement and an increase of the intensity of the Soret band. This shows that its interaction with the antibody prevents the precipitation as well as the dimerization of the cofactor **1**. When an excess of 50 μmol of sodium hydroxide is added, a displacement of the Soret band to 440 nm is observed, together with the disappearance of the maximum at 523 nm and the appearance of a maximum at 560 nm. When compared to the results obtained by Tabak and colleagues [19] with TMPyPFe, this can be explained by the formation of the monomeric porphyrin in which the iron is complexed by two hydroxyl ions. This means that when **1** is associated to the **7A3**-antibody, the axial ligands of the iron of the porphyrin change directly from aqua—to *bis*-hydroxy—without the formation of the dimeric species or precipitation of the cofactor.

3.3. Peroxidase activity

The peroxidase activity of the **1**–**7A3** complex was assayed and compared to that of the cofactor alone, using hydrogen peroxide as the oxidant and 2,2′-azino-bis(3-ethylbenzothiazoline-6-sulfonate) (ABTS) as co–substrate of the reaction. The reaction was initiated by adding hydrogen peroxide to a 500 μL solution of catalyst in presence of an excess of 500 μM ABTS, in phosphate–citrate buffer, pH 4.4.

The influence of the hydrogen peroxide concentration on the kinetics of the reaction was initially investigated. Regardless of whether the reaction was catalysed by the complex **1**–**7A3** or by **1** alone, the initial velocity increased linearly with the concentration of the oxidant in the concentration range studied (Fig. 8(a)). When measured for several concentrations of catalyst with a large excess of hydrogen peroxide (the ratio of 2.5 equivalents of antibody with respect to **1** was maintained in the case of the **1**–**7A3** complex) the initial velocity of the reaction was also found to increase linearly (Fig. 8(b)).

Despite the fact that apparently no amino-acid side chain of the antibody is chelating the iron of the porphyrin, the protein has an accelerating effect on the peroxidase activity of **1**. Indeed, in each case where the concentration of hydrogen peroxide or of catalyst was increased, the slope of the curve obtained with the initial velocity of the reaction was more than doubled with **7A3** than without it. To explain the linearity of the initial velocities with respect to hydrogen peroxide and catalyst concentrations, and to link our measurements to kinetic constants of the catalysed reaction of oxidation of ABTS, we have adapted a kinetic model, based on the one developed by Lente and Espenson [20,21] which describes the two electron oxidation of chlorophenols catalyzed by iron(III)-tetra-para-sulfonato-phenyl-porphyrin (Fe(III)TPPS). In this model, the oxidative degradation of the catalyst is taken into account, which gives the following set of equations to describe the reactions

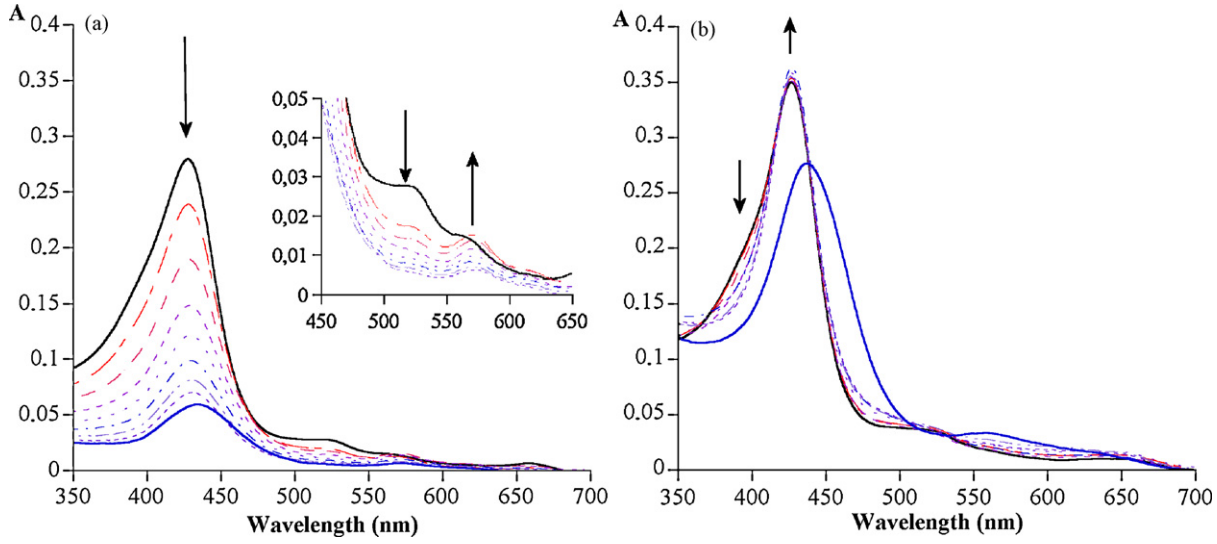

Fig. 7. Evolution of the spectra of 500 μL of a 5 μM solution of **1** and 0 μM (a) or 12.5 μM (b) of **7A3** in phosphate–citrate buffer, pH 4.4 with increasing additions of sodium hydroxide.

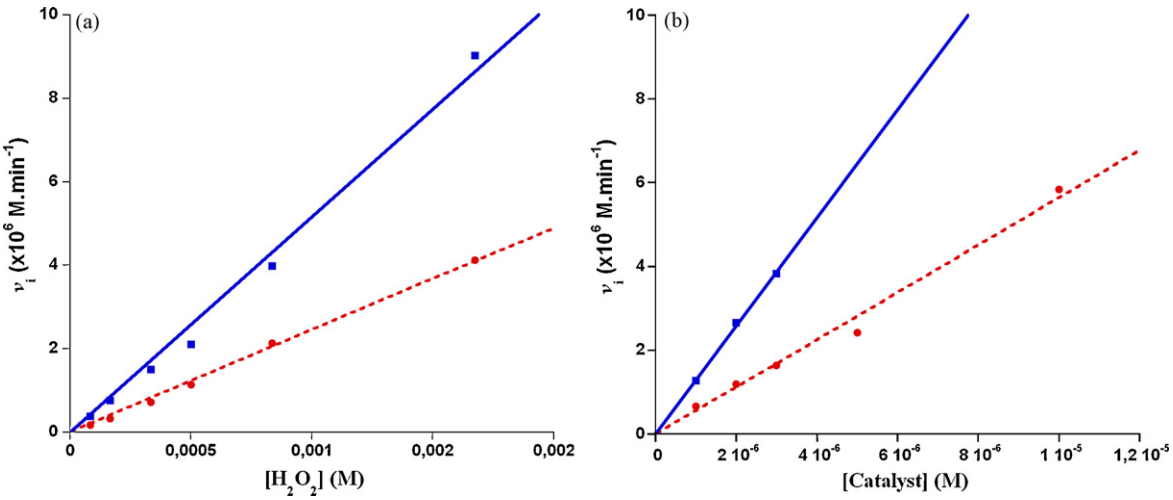

Fig. 8. (a) Plot of v_i as a function of $[H_2O_2]$ and linear regressions. [1] = 5 μM, [7A3] = 0 μM (○—dashed line) or 12.5 μM (□— plain line), [ABTS] = 500 μM. (b) Plot of v_i as a function of [Catalyst]. [7A3] = 0 (○—dashed line) or 2.5 equivalents (□—Plain line), $[H_2O_2]$ = 1.2 mM, [ABTS] = 500 μM. Phosphate–citrate buffer, pH 4.4.

involved:

$$\text{Cat} + H_2O_2 \xrightarrow{k_1} \text{Cpd I} + H_2O \qquad v_1 = k_1 \cdot [\text{Cat}] \cdot [H_2O_2] \tag{10}$$

$$\text{Cpd I} + \text{ABTS} \xrightarrow{k_2} \text{Cpd II} + \text{ABTS}^{\bullet+} \qquad v_2 = k_2 \cdot [\text{CpdI}] \cdot [\text{ABTS}] \tag{11}$$

$$\text{Cpd II} + \text{ABTS} + 2H^+ \xrightarrow{k_3} \text{Cat} + \text{ABTS}^{\bullet+} \qquad v_3 = k_3 \cdot [\text{Cpd II}] \cdot [\text{ABTS}] \tag{12}$$

$$\text{Cpd I} \xrightarrow{k_4} X \qquad v_4 = k_4[\text{Cpd I}] \tag{13}$$

The first equation describes the formation of the Compound I (Cpd I) by reaction of the porphyrin-based catalyst with hydrogen peroxide. Compound I oxidizes one molecule of ABTS to give Compound II (Cpd II), which gives the porphyrin in its ground state after oxidation of another molecule of ABTS. The last equation stands for the oxidative degradation of the catalyst. Owing to the high reactivity of compounds I and II, the standard steady-state approximation can be applied to their concentrations, which leads to the following differential equation for the concentration of the catalyst:

$$\frac{d[\text{Cat}]}{dt} = -k_4 \frac{k_1[H_2O_2]}{k_2 \cdot [\text{ABTS}] + k_4}[\text{Cat}] \tag{14}$$

At the beginning of the reaction, the variations of $[H_2O_2]$ and [ABTS] can be neglected, and the equation above gives:

$$[\text{Cat}] = [\text{Cat}]_0 \cdot e^{-k_p t} \tag{15}$$

where the pseudo first-order constant is

$$k_p = \frac{k_1[H_2O_2]_0}{(k_2/k_4)[\text{ABTS}]_0 + 1}$$

Finally, the evolution of the concentration of $ABTS^{\bullet+}$ is given by the following equation:

$$[\text{ABTS}^{\bullet+}] = 2\frac{k_2}{k_4} \cdot [\text{ABTS}]_0 \cdot [\text{Cat}]_0 \cdot (1 - e^{-k_p t}) \tag{16}$$

This relation being only valid at the beginning of the reaction, so that $[H_2O_2]$ and [ABTS] can be considered constant. The initial velocity of appearance of $ABTS^{\bullet+}$ is given by the following relation:

$$v_i = \frac{d[\text{ABTS}^{\bullet+}]}{dt}(t = 0) = 2 \cdot \frac{k_1}{[\text{ABTS}]_0 + (k_4/k_2)}[\text{ABTS}]_0[\text{Cat}]_0[H_2O_2]_0 \tag{17}$$

The value of the ratio k_2/k_4 can be estimated with Eq. (16) by extrapolation from experimental data:

$$\frac{k_2}{k_4} = \frac{[\text{ABTS}^{\bullet+}]_\infty}{2[\text{ABTS}]_0[\text{Cat}]_0} \tag{18}$$

When calculated for the two values of $[H_2O_2]$, for which hydrogen peroxide can be considered as constant, the values presented in Table 1 were obtained in the presence and in the absence of the antibody.

The value of k_2/k_4 calculated in the presence of the antibody is only slightly higher than that in the absence of the protein. The results obtained with the sulfoxidation of thioanisole have shown a protective effect of the protein on the catalyst [12] which suggests that the steric hindrance generated by the protein around the porphyrin might slow down the reaction of ABTS with Compound I by restricting the access to the catalytic center. With the values of k_2/k_4 calculated, the kinetic constant k_1 of the reaction between the catalyst and hydrogen peroxide can be obtained from the slope of the curves of v_i as a function of $[H_2O_2]_0$ and $[Cat]_0$ given by the following relation derived from Eq. (17):

$$k_1 = \frac{([\text{ABTS}]_0 + (k_4/k_2)) \cdot v_i}{2 \cdot [\text{ABTS}]_0[\text{Cat}]_0[H_2O_2]_0} \tag{19}$$

The values of k_1 computed from the two sets of experiments are roughly the same, when taking into account the experimental errors (Table 1). These values of k_1 explain why the velocity of the formation of $ABTS^{\bullet+}$ is much higher in the presence of the protein. The antibody seems to have mainly an accelerating effect on the kinetics of the reaction of hydrogen peroxide with the iron(III)-porphyrin, which is increased more than 2.2 times. The fact that the accelerating effect of the antibody occurs in a step of the reaction which involves only hydrogen peroxide and the iron–porphyrin shows that the influence of the protein is due to amino acids located close enough to the porphyrin ring, rather than an interaction with the co-substrate ABTS.

Table 1
Average values calculated for the ratio of kinetic constants k_2/k_4 for different hydrogen peroxide concentrations, and for the kinetic constant k_1, in the presence and in the absence of the antibody.

	1	1–7A3
k_2/k_4 (M^{-1})	32,280	33,980
k_1 (M^{-1} min^{-1}) $[H_2O_2]$ var.	268	577
k_1 (M^{-1} min^{-1}) [Cat] var.	250	570
k_1, mean value (M^{-1} min^{-1})	259 ± 9	574 ± 4

4. Conclusions

In conclusion, this study has highlighted several important data concerning the artificial metalloenzyme built by association of the estradiol–iron–porphyrin conjugate **1** with the antibody **7A3**. First, the estradiol moiety of the cofactor is effectively recognized by the antibody, as shown by the titration experiment. The dissociation constant determined for the **1**–**7A3** complex is still very low ($K_D = 4 \times 10^{-7}$ M) despite the porphyrin being linked to the estradiol. This allows us to consider that above micromolar concentrations, and in the presence of an excess of antibody, all the cofactor is strongly anchored into the recognition pocket of the protein.

The coordination experiments performed with imidazole on the **1**–**7A3** complex have shown that the iron of the porphyrin can still accommodate two imidazole molecules, which means that the protein generates only a weak steric hindrance around the macrocycle.

However weak, this steric hindrance exists, since the comparison of the C_{50} measured to that of a free, non μ-oxo dimer forming porphyrin, as well as the absence of dimerization when raising the pH in the presence of the antibody are evidence for a presence of the protein around the porphyrin.

The artificial metalloenzyme displays a two-fold increase in peroxidase activity compared to the unbound cofactor. The kinetics studies have shown that this increase in activity is due to the rate of formation of the high valent iron–oxo species k_1, which also increases by a factor of 2 in the presence of the antibody. This could be explained by the participation of the side chain of an amino acid of the protein to the heterolytic cleavage of the O–O bond of H_2O_2, in agreement with the evidence of steric hindrance brought by the protein around the porphyrin.

This study validates the strategy of associating an antibody with an antigen-based cofactor by the so-called "Trojan horse" strategy to lead to artificial metalloenzymes with a peroxidase activity. Indeed, the protein still retains good affinity for its antigen, even when linked to such a bulky molecule as a porphyrin, and interacts closely enough with the catalytic center to influence its activity.

On the basis of these results, we aim to build new artificial metalloenzymes, based on the same scaffold. To improve the catalyst's activity, other water-soluble metalloporphyrins and different metal centers, such as manganese for example, will be used to lead to artificial metalloenzymes performing other reactions such as alkene epoxidation and alkane hydroxylation. Finally, improved selectivities may be achieved using spacers of variable lengths between the antigen and the macrocycle, to modify the environment of the porphyrin.

References

[1] P.T. Anastas, M.M. Kirchhoff, Acc. Chem. Res. 35 (2002) 686.
[2] M. Hamid, Khalil-ur-Rehman, Food Chem. 115 (2009) 1177.
[3] S. De Lauzon, D. Mansuy, J.-P. Mahy, Eur. J. Biochem. 269 (2002) 470.
[4] R. Quilez, S. De Lauzon, B. Desfosses, D. Mansuy, J.-P. Mahy, FEBS Lett. 395 (1996) 73.
[5] R. Ricoux, E. Lukowska, F. Pezzotti, J.-P. Mahy, Eur. J. Biochem. 271 (2004) 1277.
[6] R. Ricoux, R. Dubuc, C. Dupont, J.-D. Marechal, A. Martin, M. Sellier, J.-P. Mahy, Bioconjugate Chem. 19 (2008) 899.
[7] R. Ricoux, M. Allard, R. Dubuc, C. Dupont, J.-D. Marechal, J.-P. Mahy, Org. Biomol. Chem. (2009), 10.1039/b907534 h.
[8] M.E. Wilson, G.M. Whitesides, J. Am. Chem. Soc. 101 (1978) 306.
[9] J. Collot, J. Gradinaru, N. Humbert, M. Skander, A. Zocchi, T.R. Ward, J. Am. Chem. Soc. 125 (2003) 9030.
[10] A. Pordea, M. Creus, J. Panek, C. Duboc, D. Mathis, M. Novic, T.R. Ward, J. Am. Chem. Soc. 130 (2008) 8085.
[11] S. De Lauzon, B. Desfosses, M.-F. Moreau, N. Le Trang, K. Rajkowski, N. Cittanova, Hybridoma 9 (1990) 481.
[12] Q. Raffy, R. Ricoux, J.P. Mahy, Tetrahedron Lett. 49 (2008) 1865.
[13] E.N. Kadnikova, N.M. Kostić, J. Mol. Catal. B 18 (2002) 39.
[14] A.G. Cochran, P.G. Schultz, J. Am. Chem. Soc. Chem. 112 (1990) 9414.
[15] D. Brault, M. Rougee, Biochem. Biophys. Res. Commun. 3 (1974) 654.
[16] Ö. Almarsson, H. Adalsteinsson, T.C. Bruice, J. Am. Chem. Soc. 117 (1995) 4524.
[17] G.M. Miskelly, W.S. Webley, C.R. Clark, D.A. Buckingham, Inorg. Chem. 27 (1988) 3773.
[18] F.L. Harris, D.L. Toppen, Inorg. Chem. 17 (1978) 71.
[19] S.C.M. Gandini, E.A. Vidoto, O.R. Nascimento, M. Tabak, J. Inorg. Biochem. 94 (2003) 127.
[20] G. Lente, J.H. Espenson, Int. J. Chem. Kinet. 36 (2004) 449.
[21] G. Lente, J.H. Espenson, New J. Chem. 28 (2004) 847.